

## AQUEOUS NANOEMULSIONS IN FUELS: A CORROSION STUDY

A. ROSAS-JUÁREZ<sup>a,b</sup>, V. M. CASTAÑO<sup>a\*</sup>

<sup>a</sup>*Centro de Física Aplicada y Tecnología Avanzada, UNAM, Boulevard Juriquilla 3001, Querétaro, Qro. 76230, México*

<sup>b</sup>*Facultad de Ciencias Químicas, Benemérita Universidad Autónoma de Puebla Apdo. Postal J-55, Puebla, Pue. 72570, México*

A new surfactant (SCFATA, developed in our group) was employed to prepare aqueous nanoemulsions in commercial automobile gasolines. The surfactant is completely miscible in water and oil. Stable nanoemulsions, nearly monodisperse, were attained without cosurfactant and with moderate stirring. SCFATA is also an octane enhancer as tested in a two-cycles engine. The effect of the high water content (up to 95%) in the aqueous nanoemulsion in gasolines on the corrosion performance of a API X-80 pipeline steel, in both static and dynamic conditions, was studied by dynamic polarization and linear polarization resistance.

(Received April 16, 2016; Accepted June 10, 2016)

*Keywords:* Surfactant, Gasoline, Corrosion, Nanoemulsion.

### 1. Introduction

Altern fuels constitute an attractive research area for the development of new fuels with enhanced properties. In particular, altern fuels are promising fuels for better air-quality problems in order to reduce emissions of carbon monoxide and other pollutants from automobiles. The quality of oxygen that must be added is dependent upon the severity of the air quality problem. "Reformulated" gasolines, containing a minimum of 2% oxygen by weight are most commonly required while "oxygenated" gasolines containing 2.7% or more of oxygen may be required in the winter months for the most problematic urban areas. The chemical oxygenates most commonly added to these "reformulated" gasolines include methyl tert-butyl ether (MTBE) and ethanol. Of these, MTBE use exceeds that of ethanol. However, the use of ethanol is expected to increase in United States due to potential health effects associated with MTBE and market forces (New York Times (1997), Cook et al. (2011)). Also, the pollution in different industries, by using gasoline and diesel, is revealing more and more complex pollutants (Reda et al. (2014)) In order to meet the fuel mandates, reformulated gasolines must contain 5.5% ethanol by volume and oxygenated fuels must contain 7.4% ethanol. Ethanol is also added to gasolines as an alternative replacement for petroleum compounds. Automobiles are currently being manufactured that may use fuel containing ethanol fractions as high as 85%. The presence of MTBE, ethanol and other chemical oxygenates in gasolines has prompted concern among scientists and environmental compartments, including groundwater and snow (Pouloupoulos et al. (2000), Kolb et al. (2006)). Oxygenates, especially alcohols, can act as a cosolvent and significantly increase the aqueous solubility of potentially harmful hydrocarbons. In a subsurface gasoline spill scenario, the increase the potential for human exposure to these chemicals (Heermann et al. (1998); Bravo et al. (2000); Uri et al. (1999); Schifter et al. (2001); Pinal et al. (1990), Groves (1988); Cline et al. (1991); Stephenson. (1992), Oliverira et al. (2007), Pereda et al. (2009)). Ethanol is also added to gasolines as an alternative replacement for petroleum compounds. Automobiles are currently being manufactured that may use fuel containing ethanol fractions as high as 85%. Some studies focused on the potentially detrimental hygroscopic nature of oxygenated gasolines in automobile engines. (Letcher et al. (1986), Lojkásek et al. (1992), Ginnebaugh et al. (2010)).

---

\*Corresponding author: meneses@unam.mx

Emulsions are dispersions of one liquid in other in a form of droplets of sizes usually ranging between 0.1 to 10  $\mu\text{m}$  (Solans et al. (20056), Juarez et al. (2008)). If the average particle size is within the 0.01 to 0.1  $\mu\text{m}$  interval, the system is called a microemulsion. They is even a visual distinction: microemulsions are crystal clear whereas standard emulsions have a cloudy appearance, because of differences in light scattering.

The two phases of emulsions are completely or partially immiscible and the dispersion is stabilized by surfactants, including the stabilization by small solid particles. In some systems, the addition of a fourth component, a cosurfactant, to an oil-water-surfactant system can cause the interfacial tension to drop to near-zero values, easily on the order of  $10^{-3}$  to  $10^{-4}$  mN/m; low interfacial tension allows spontaneous, or nearly spontaneous, emulsification down to very small droplet sizes, ca. 10 nm or even smaller. The droplets can be so small that they scatter light weakly; the emulsions appear to be transparent and do not break under neither standing or centrifugation. Unlike coarse emulsions, these microemulsions are usually thought to be thermodynamically stable.

The recent interest of the scientific community worldwide on nanotechnology has led to a renewed interest on the scientific and technological aspects of the production of even smaller emulsion sizes: nanoemulsions. The self-organization of mesoscopic superstructures such as membranes, tubes, sponges, and so forth with a characteristic nanometer-length scale is expected to open up a rich path for the so-called “bottom-up” approach, which is supposed to complement or even replace the current “top-down” device fabrication technology in the near future. (Heermann et al. (1998), da Silva et al. (2013)).

On the other hand, a severe limitation to the practical use of standard or micro aqueous emulsions in oil and/or fuels is the corrosion behavior, which could be catastrophic due to the complex interfacial phenomena at the interfaces fuel-water-pipeline.

The aim of the present work is to study a electrochemical method for corrosion testing will be used with fuels containing various percentages of water added as nanodroplets, by using a novel surfactant SCFATA, developed in our group.

## 2. Experimental

**Materials.** Commercial mexican gasoline Pemex Magna (regular) and Pemex Premium were used as sold by the state-owned oil company. API X-80 pipeline steel having 0.013(wt%) C, 1.52 Mn, 0.05 Mo, 0.007 P, 0.038 Nb, 0.009 S, 0.20 Si, 0.1 V, 0.028 Al, 0.005 Ti, 0.21 Ni, 0.11 Cr-Fe(bal) was used.

**Techniques.** A volumetric method was used to obtain aqueous nanoemulsions in gasolines. They were obtained from binary samples of water-fuel with 5%-95% concentration per volumen of water.at 4°C and 25°C. Particle size was determined by a Malvern Autosizer 4800 equipped with a laser model Innova Coherent 90K. Electrochemical experiments were performed using a Gamry Instruments PC3 potentiostat controlled by an CMS100 software. Octane index was determined with CFR machines and the ASTM norms were used to RON and MON numbers: ASTM-D-2699 and ASTM-D-2700 respectively.

Aqueous nanoemulsions in fuels were used in internal combustion motor of two cycles. Technical data of the machine are shown in Table 1.

*Table 1. Technical data to internal combustion monocylindrical motor of 2 cycles.*

Rolling:	27.2 cm <sup>3</sup>
Stroke	30.0 mm
Diameter	34.0 mm
Power as ISO 8893	0.75 kW (1 CV)
Ralenti regime	2800 rpm
Regime max. of motor	9500 rpm
Regime max of tree to operate	9500 rpm

**Synthesis of nanoemulsions in fuels and phase diagrams.** Phase diagrams were obtained for the system based on gasoline 87 octane grade (Regular), and the system based on gasoline 93 octane grade (Premium) at a fixed temperature by careful addition of the surfactant SCFATA to a exactly-measured mixture of gasoline and water by using a micropipette in a 125 cm<sup>3</sup> flask. The surfactant SCFATA was added using a burette. The flask was carefully shaken in a controlled waterbath and drops added until one drop of surfactant caused the cloudy solution to become clear.

The results were checked by measured volume exact of gasoline, water and surfactant, (mixtures that corresponded to points on the binodal curve) into flasks which were sealed. The flasks were then shaken in a waterbath and the temperature slowly adjusted until the clear solution occurred.

Aqueous nanoemulsions in gasolines were obtained from binary samples of water-fuel with 5%-95% concentration per volumen of water. Nineteen stable base emulsions containing destilated water, gasoline Pemex Magna, and gasoline Pemex Premium were formulated using SCFATA surfactant. Pemex Magna and Pemex Premium gasolines, and destilated water were used as supplied. The phase diagrams were repeated three times over a period of 13 months and no measurable difference could be found in the results, indicating that the water nanodroplets-surfactant-gasoline composition were stable over that period

#### **Scheme 1.** Electrochemical experiments

The relevant experimental parameter for the electrochemical technique were:

- a) Lineal polarization resistance (Rp): potentiostatic, potential range  $\pm 0.01$  V (referred to the  $E_{\text{corr}}$ ), potential scanning rate=0.017 mVs<sup>-1</sup>.
- a) Polarization curves: at a rotation rate of 0 rpm a cathodic and an anodic polarization curves were measured on different steel samples. Before the experiments, the  $E_{\text{corr}}$  value was measured during 30 minutes approximately until it was stable. These polarization curves were obtained, departing from  $E_{\text{corr}}$ , at a scanning rate of 0.005Vs<sup>-1</sup>, in cathodic or anodic direction, depending on each case. Therefore, two polarization curves were obtained, one cathodic and one anodic. Before the experiments, the  $E_{\text{corr}}$  value was measured during 30 minutes approximately until it was stable. At a rotation rate of 400 rpm a single polarization curve was obtained after 4 hours of exposure time, at each water concentration. In this particular case, the polarization curves were started at an overpotential of  $-800$  mV (with respect to  $E_{\text{corr}}$ ) and stopped at an overpotential of  $+1500$ mV (referred to  $E_{\text{corr}}$ ). All the potentials were measured using a Saturated Calomel Electrode (SCE) as reference electrode coupled to a Luggin probe (Khaouei et. Al (2014)). The counter electrode was a platinum wire (Zhu et al. (2010)). Corrosion rates were calculated by using Tafel extrapolation, for the case of the polarization curves, and by using polarization resistance, Rp, obtained from Tafel slopes. All tests were performed at room temperature ( $25^{\circ}\text{C}\pm 2^{\circ}\text{C}$ ).

#### **Scheme 2.** Octane Index

Octane index was determinated with CFR machines and the ASTM norms were used to RON and MON numbers: ASTM-D-2699 and ASTM-D-2700 respectively.

#### **Scheme 2.** Performance of aqueous nanoemulsions

Aqueous nanoemulsions in fuels were used in internal combustion motor of two cycles. Technical data of the machine are shown in Table 1.

### **3. Results and discussion**

Points on the binodal curves (Figure. 1) were determined as described above, showing the narrow region that allow the stabilization oif nanodroplets in water by using the new surfactant. Polarization curves for X-80 steel in water in Pemex Magna gasoline+SCFATA nanoemulsions at different water content are shown in Figures 2, 3, 4 and 5. It can be seen that both anodic and cathodic current densities in static conditions incese as follows: M7-4C 35% $\text{H}_2\text{O}$ , M3-4C

15% $H_2O$ , M13-4C 65% $H_2O$ , M1-4C 5% $H_2O$ , M9-4C 45% $H_2O$ , M11-4C 55% $H_2O$ , M5-4C 25% $H_2O$ , M17-4C 85% $H_2O$ , M19-4C 95% $H_2O$ , M15-4C 75% $H_2O$ , and it can be seen that both anodic and cathodic densities in dynamic conditions increase as follows: M1-4C 5% $H_2O$ , M7-4C 35% $H_2O$ , M5-4C 25% $H_2O$ , M13-4C 65% $H_2O$ , M3-4C 15% $H_2O$ , M11-4C 55% $H_2O$ , M9-4C 45% $H_2O$ , M17-4C 85% $H_2O$ , M19-4C 95% $H_2O$ , M15-4C 75% $H_2O$ . In all cases % $H_2O$  represents the percent in volume of water in binary mixture gasoline-water, and 4C indicates that samples were prepared at 4°C.

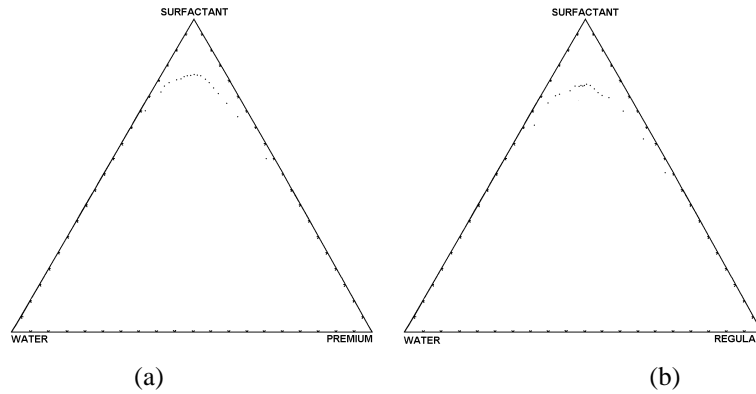


Fig. 1. Isotermis for systems of fuel-water mixtures containing (a) gasoline 87 octane grade (Regular), (b) gasoline 93 octane grade (Premium) at 25°C.

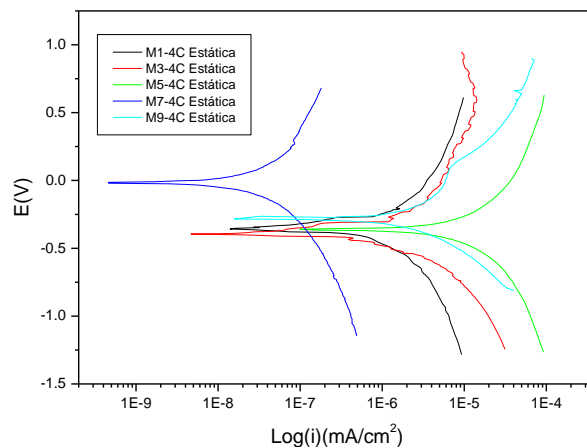


Fig. 2. . Polarization curves in static conditions for aqueous nanoemulsions in Pemex Magna gasoline-SCFATA.

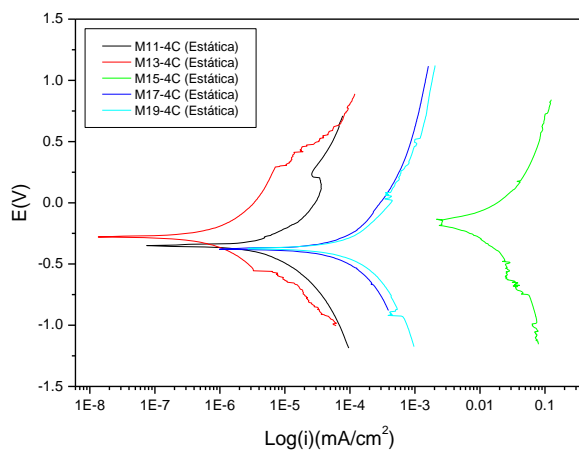


Fig. 3. Polarization curves in static conditions for aqueous nanoemulsions in Pemex Magna gasoline-SCFATA

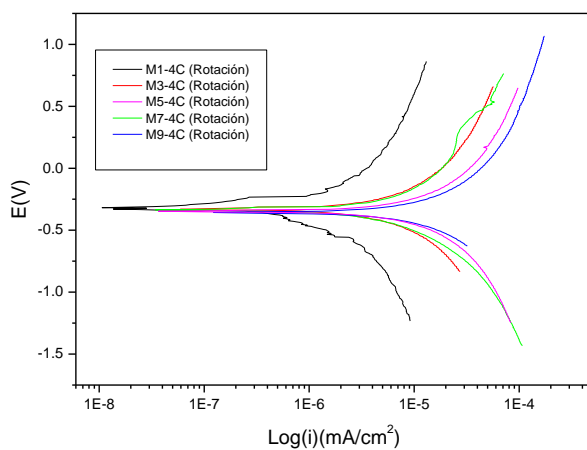


Fig. 4. Polarization curves in dynamic conditions for aqueous nanoemulsions in Pemex Magna gasoline-SCFATA.

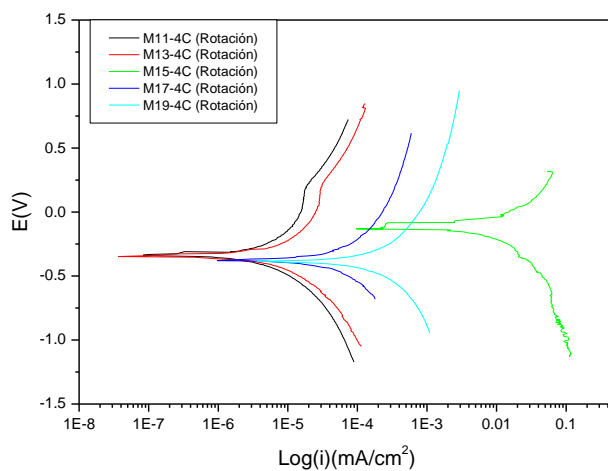


Fig. 5. Polarization curves in dynamic conditions for aqueous nanoemulsions in Pemex Magna gasoline-SCFATA.

No passive region was found for all gasoline contents, however, in static conditions (Fig. 2 and 3), the corrosion current density is lower than in dynamic conditions (Fig. 4 and 5) in samples: M7-4C, M3-4C, M13-4C, M1-4C and M19-4C. Nevertheless, M7-4C and M3-4C samples are bigger than in dynamic conditions. In dynamic conditions the corrosion current density is bigger than in static condition in samples: M9-4C, M5-4C and M15-4C. But the M11-4C and M17-4C samples have the same corrosion current density in both that static and dynamic conditions.

The variation of corrosion current density,  $I_{corr}$  with time and aqueous nanoemulsions in gasoline Pemex Magna concentration, at 0 rpm is shown in Figure 6, which demonstrates the dependence of the measured corrosion current density with water concentration. Indeed, as the water concentration increases the measured corrosion rate increases, as it could be expected. It is interesting to notice the following feature at the beginning of the experiment:  $I_{corr}$  decreases with time and then reaches a steady value. This can be observed in the M19-4C, M17-4C, M15-4C samples. It is interesting too, that at the 1000, 1800 and 2000 seconds of the experiment,  $I_{corr}$  increases with time and then decreases to a steady value. This can be observed in M3-4C, M15-4C and M19-4C samples. However, for the M17-4C sample, the tendency for  $I_{corr}$  is to decrease at the beginning of the experiment to a steady state value, but then decrease to new a steady value.

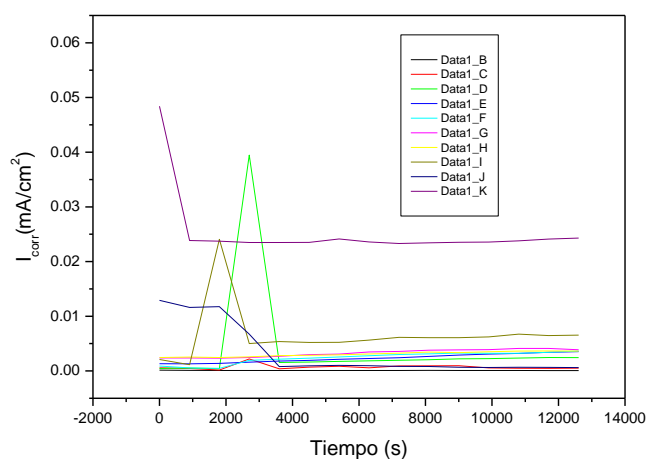


Fig. 6. Corrosion current density,  $I_{corr}$  vs time for aqueous nanoemulsions in gasoline Pemex Magna at 0 rpm.

Fig 2 demonstrates that, at 0 rpm,  $I_{corr}$  is independent of the surfactant, and water concentration. The calculated values of  $I_{corr}$  are practically the same, at bulk concentrations of surfactant and water (except M19-4C sample). These results indicate that, static conditions favours the SCFATA surfactant migration, from the bulk of the solution, towards the surface of the electrode. This increased migration rises the SCFATA surfactant concentration and coverage at the surface of the electrode, thus decreasing  $I_{corr}$ .

The surfactant SCFATA is miscible completely with water for all five gasolines prepared and tested.

The effect of temperature on the binodal curves for two systems (water-gasoline Pemex Magna-SCFATA and water-gasoline Pemex Premium-SCFATA) at 4°C and 40°C can be observed in Figures 7 and 8, respectively.

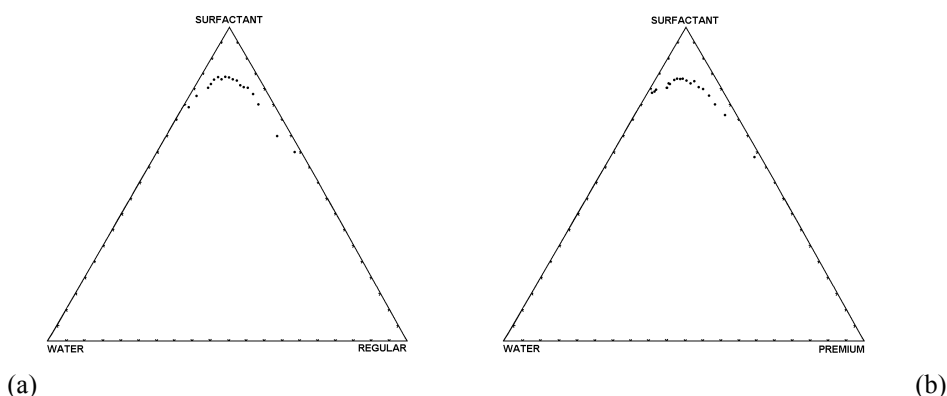


Fig. 7. Isotherms for fuel-water mixtures containing (a) gasoline 87 octane grade (Regular), (b) gasoline 93 octane grade (Premium) at 4 °C.

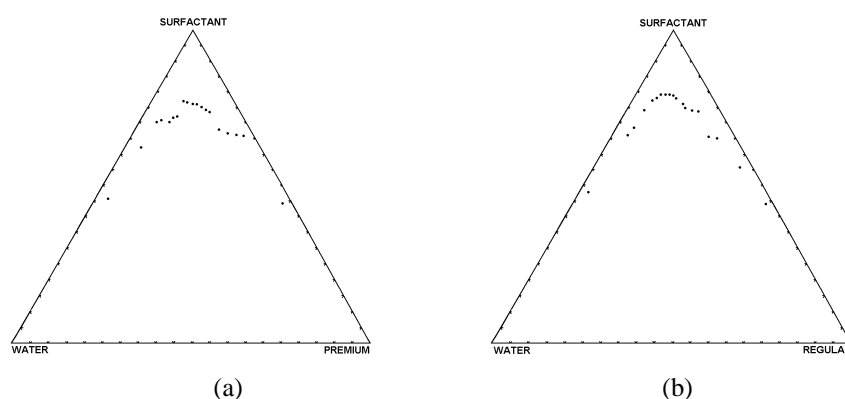


Fig. 8. Isotherms for fuel-water mixtures containing (a) gasoline 87 octane grade (Regular), (b) gasoline 93 octane grade (Premium) at 40 °C.

Figs. 8 and 9 show that the surfactant in the blend has a significant effect on the solubility of water. Samples of nanoemulsions, stored in sealed amber bottles at room temperature, were monitored over a period of two years approximately, showing a remarkable stability.

Octane index was determined from Pemex Premium and Pemex Magna gasolines only to following samples: M1-4C, P1-4C, P5-4C, and Pemex Premium gasoline in octane machines with certainty of 95.451. RON and MON proof is made with ASTM norm: ASTM-D-2699 (RON) and ASTM-D-2700 (MON). Results are shown in Table 2. Same results were obtained of mixtures with 50% in volume of n-heptane. But the P5-4C sample (Pemex Premium gasoline nanoemulsion) with 75% in volume of n-heptane showed an octane index of 91. Then, theoretically the P5-4C nanoemulsion has an octane index of 273. This result mean that the SCFATA surfactant to be able to used as octane-boosting blend component. The surfactant SCFATA has high octane ratings and hence is attractive substitute for oxygenated hydrocarbons such as ethers are used as so-called octane-boosting blend components in order to preserve the octane quality of gasoline.

Table 2. Determination of RON and MON numbers, octane index and uncertainty with CFR machines.

Sample	RON	i	MON	i	I.O.
Pemex Premium	97.2	±0.16	88.1	±0.16	92.65
M1-4C	N/D	N/D	N/A	N/D	N/A
P1-4C	N/D	N/D	N/A	N/D	N/A
P5-4C	N/D	N/D	N/A	N/D	N/A

Where N/D= no determined; N/A= no applied i= uncertainty; I.O.= octane index

Aqueous nanoemulsions in fuels were used in a two-cycles internal combustion. Results are shown in Tables 3 and 4, demonstrating a good behavior as fuels.

Table 3. Performance of aqueous nanoemulsions in Pemex Premium gasoline for a 2-cycles single cylinder engine.

Fuel	Volume (mL)	Operate time (min)	Efficiency (attempts before start of the engine)
Premium	100	≈15	11
P1-4C	100	≈15	8
P2-4C	100	≈13	13
P3-4C	100	≈15	11
P4-4C	100	≈15	11
P5-4C	100	≈13	14
P6-4C	100	≈13.5	12
P7-4C	100	≈15	13
P8-4C	100	≈14	18
P9-4C	100	≈14	22
P10-4C	100	≈13.5	20
P11-4C	100	≈14	24
P12-4C	100	≈15	35

Table 4. Performance of aqueous nanoemulsions in Pemex Magna gasoline for a 2-cycles single cylinder engine.

Fuel	Volume (ml)	Operate time (min)	Efficiency (attempts before start of the engine)
Magna	100	≈16	7
M1-4C	100	≈15.5	7
M2-4C	100	≈15	11
M3-4C	100	≈15	9
M4-4C	100	≈14	15
M5-4C	100	≈14	15
M6-4C	100	≈13	17
M7-4C	100	≈13.5	15
M8-4C	100	≈13	19
M9-4C	100	≈13.5	22
M10-4C	100	≈13	26
M11-4C	100	≈13	29

#### 4. Conclusions

The preparation of aqueous emulsions in fuels using SCFATA surfactant makes easy the blend between water and gasolines. Our results indicate that the nanoemulsions are transparent dispersions, stables and none cosurfactant was required. The emulsification process no required a considerable amount of mechanical energy. The average particle size is on the order of nanometers. This new nanoemulsions have properties of carburetant and we was given possibility to apply as altern fuels. Preliminary results exist that the SCFATA surfactant to be able to used as octane-boosting blend component. The corrosion behavior of API X-80 pipeline steel in aqueous nanoemulsions in fuels under static and dynamic conditions has been studied using polarization curves and corrosion potential versus time curves techniques. These techniques were found to be effective in assessing the corrosion behavior of this steel in nanoemulsions, and they were sensitive to the water contents generally, reaching a maximum value in M15-4C sample. No passive region was found for all gasoline contents, however, generally in static conditions the corrosion current density is lower than dynamic conditions. Nevertheless, the water contents is high, the corrosion rate is to decrease at the beginning of the experiment to a steady value.

#### References

- [1] V. Balan, D. Chiramonti, S. Kumar, *Biofuels, Bioprod. Bioref.* **7**, 732 (2013).
- [2] V. Balan, *Biotechnology* 1-31 (2014)
- [3] H.A. Bravo, R.J. Torres *Atmospheric Environment* **34**, 499 (2000).
- [4] P. V. Cline, J. J. Delfino, P. S. C. Rao, *AICHE J.* **21**(6), 1086 (1991)
- [5] G. Carbajal, M. Espinosa, A. Martínez, G. González, V.M. Castaño, *The Open Corrosion Journal* **2**, 197 (2009)
- [6] M. Canakci, Ahmet Necati Ozsezen, Ertan Alptekin, Muharren Eyidogan. *Renewable Energy* **52**, 11 (2013)
- [7] R. Cernansky, *Nature* **519**, 379 (2015).
- [8] R. Cook, S. Phillips, M. Houyoux, P. Dolwick, R. Mason, C. Yanca, M. Zawacki, K. Davidson, H. Michaels, C. Harvey, J. Somers D., Luecken, *Atmospheric Environment* **45**, 7714 (2011).
- [9] M.L.B. Da Silva, D.E. Gomez, P.J.J. Alvarez, *Journal of Contaminant Hydrology* **146**, 1 (2013).
- [10] A. Demirbas, *Applied Energy* **88**, 17 (2011)
- [11] M. A. Deyab, *Corrosion Science.* **80**, 359 (2014)
- [12] D.L. Ginnebaugh, J. Liang, M.Jacobson, *Atmospheric Environment* **44**, 1192 (2010).
- [13] F. R., Groves, *Environ. Sci. Technol.* **22**(3), 282 (1988)
- [14] S.E. Heermann, S.E. Powers *Journal of Contaminant Hidrology* **34**, 315 (1998)
- [15] A. Juarez, A.L. Rivera, V.M. Castaño, *Nanotrends* **4**, 1 (2008)
- [16] A. Khajouei, E. Jamalizadeh, A.H. Jafari, S.M.A. Hosseini, *Corrosion Engineering, Science and Technology*, **49**, 743 (2014)
- [17] A. Kolb, W. Püttmann, *Atmospheric Environment* **40**,76 (2006)
- [18] T.M. Letcher, C. Heyward, S. Wootton, B. Shuttleworth *Fuel* **65**, 891(1986)
- [19] M. Lojkásek, V. Ruzicka Jr., A. Kohoutová., *Fluid Phase Equilibria* **71**(1), 113 (1992)
- [20] *New York Times.* (1997) *New York Times*, June 4, 1997, pp. A1, D4.
- [21] R. Pinal, P. S. C., Rao, L. S., Lee, P. V., Cline, S. H., Yalkowsky, *Environ. Sci. Technol.* **24**(5), 639 (1990).
- [22] M.B. Oliveira, J.P.A. Coutinho, A.J. Queimada, *Fluid Phase Equilibria* **258**, 58 (2007)
- [23] S., Pereda, J.A., Awan, A.H., Mohammabi, A., Valtz, C., Coquelet, A.A., Brignole, D. Richon, *Fluid Phase Equilibria* **275**, 52 (2009)
- [24] S., Pouloupoulos, C. Philippopoulos, *Atmospheric Environment* **34**, 4781 (2000)
- [25] A.A., Reda, J., Schnelle-Kreis, J., Orasche, G., Abbaszade, J., Lintelmann, J.M., Arteaga-Salas, B., Stengel, R.,Rabe, H., Harndoff, O. Sippula, T. Streibel, R. Zimmermann, *Atmospheric Environment* **94**, 467 (2014)

- [26] D. P. Rimmer, A.A. Gregoli, J. A. Hamshar, E. Yildirim, In Pipeline Emulsion Transportation for Heavy Oils. Schramm L. L., Ed.;Advances in Chemistry Series 231;American Editor) American Chemical Society, Washington, DC (1992).
- [27] I. Schifter, M. Vera, L. Díaz, E. Guzmán, F. Ramos, E. López-Salnas Environ. Sci. Technol..**35**(10), 1893(2001)
- [28] C., Solans, P., Izquierdo, J., Nolla, N., Azemar, N.J. Garcia-Zelma, Current Opinion in Colloid and Interface Science **10**, 102 (2005)
- [29] R. M. Stephenson, J. Chem. Eng. Data. **37**(1), 80 (1992).
- [30] N.D. Uri, R.J. Boyd Journal of Policy Modeling **21**, 527 (2000)
- [31] M. Yada, J. Yamamoto, H. Yokoyama, Langmuir, **18**, 7436 (2002)
- [32] Y.L. Zhu, X.P. Guo, Y.B. Qiu, Corrosion Engineering, Science and Technology **45**, 442 (2010).